Persistent viral infections impact key biological traits in *Drosophila melanogaster*

Mauro Castelló-Sanjuán[1], Rubén González[1], Ottavia Romoli[1], Hervé Blanc[1], Jared Nigg[1, #], Maria-Carla Saleh[1].

[1]Institut Pasteur, Université Paris Cité, Viruses and RNA Interference Unit, Paris, France.

[#]Current address: Chan Zuckerberg Biohub, San Francisco, California, USA.

Correspondence: jared.nigg@czbiohub.org, carla.saleh@pasteur.fr

Short title: Consequences of persistent viral infections

ABSTRACT

Persistent viral infections have been assumed to have minimal fitness costs for insects. Using *Drosophila melanogaster*, we established persistent mono-infections with four different enteric RNA viruses (Drosophila A virus, Drosophila C virus, Bloomfield virus, and Nora virus) and observed that these infections significantly reduce fly survival, alter the number of viable offspring per female, modulate microbiome composition, and impact locomotor abilities. These results demonstrate significant impacts of persistent viral infections on key biological traits and challenge the assumption of the innocuity of persistent viral infections for the host. In addition, the four viruses displayed different accumulation kinetics and elicited unique transcriptional profiles with no common core responses. The transcriptional changes triggered by DCV infection persisted even after viral clearance. Our findings reveal that persistent viral infections modulate critical aspects of insect biology and can have negative impacts on host physiology and behavior.

INTRODUCTION

The increasing availability of sequencing data has revealed tens of thousands of novel viruses in multiple host organisms, suggesting the widespread occurrence of previously undetected infections (Ho & Tzanetakis, 2014; Kapun *et al.,* 2020; Wallace *et al.,* 2021). In some cases, these are persistent infections that represent a metastable state in which the physiological impacts of viral infection are maintained below a lethal threshold without leading to viral clearance (Goic & Saleh 2012). In contrast to acute viral infections, which are characterized by rapid viral replication that is ultimately limited by the death of the host or clearance of the virus, persistent infections endure over extended periods within the individual host. During this time, the virus is still capable of being transmitted to other organisms or the host's offspring despite the inherent limitations imposed by the host's immune responses and cellular mortality (Goic & Saleh 2012).

Persistence is a frequent phenomenon in viral infections across all kingdoms, as it can provide advantages for both the virus and the host, acting as a modulator of the ecosystem. For example, livestock and crops often suffer from infections caused by harmful or deadly viruses (Goic & Saleh 2012). Growing evidence shows that persistent infections have costs to the host (Nigg et al. 2024, Wallace and Obbard, 2024). Nevertheless, research has mostly focused on the acute effects of viral infections. Consequently, the impacts of persistent infections on host physiology and behavior remain understudied.

In this study, we aimed to shed light on the consequences of persistent infections using the fruit fly, *Drosophila melanogaster*. This insect has an extensively characterized genome and short generation times, making it an ideal model organism for studying persistent viral infections throughout its lifespan. In a previous study, we demonstrated

47 that persistent infections with natural viruses are associated with decreased lifespan in
48 *D. melanogaster* (Nigg *et al.,* 2024). In the present study, we aimed to further examine the
49 effects of persistent mono-infections with four distinct enteric RNA viruses—Drosophila
50 A Virus (DAV), Drosophila C Virus (DCV), Bloomfield virus, and Nora virus —on a wide
51 range of physiological traits in *D. melanogaster*. Specifically, we focused on survival
52 rates, fertility (reproductive output, here defined as the number of viable offspring),
53 bacteriome composition, and locomotor abilities. These traits are essential for
54 understanding the host's overall fitness and its ecological interactions. Survival rates and
55 reproductive output serve as key indicators of an organism's ability to thrive and
56 contribute to the next generation (Crone, 2001). The composition of the microbiome has
57 been observed to influence various aspects of the host's physiology, such as nutrition
58 status, immune function, behavior, and overall health (Gould *et al.,* 2018; Jia *et al.,* 2021;
59 Shin *et al.,* 2011; Tafesh-Edwards & Eleftherianos, 2023). Locomotor abilities are vital for
60 behaviors such as foraging, mating, and avoiding predators, all of which are crucial for
61 survival and reproduction (Irschick and Garland, 2001). By examining these traits, we
62 aimed to elucidate the broader implications of persistent viral infections on insect
63 biology.
64
65 **RESULTS**
66 **The dynamics of viral RNA levels over time are virus specific**
67 Our laboratory has previously established persistent viral mono-infections in *D.*
68 *melanogaster* flies of the w^{1118} genetic background using different viruses: DAV, DCV,
69 Bloomfield virus, and Nora virus (Nigg *et al.,* 2022, 2024). All these viruses naturally infect
70 *D. melanogaster* and are transmitted primarily through orofecal contamination. In this

71 work, we measured key biological traits over time in the infected populations and an
72 uninfected control population (Figure 1A). To maintain continuous exposure to
73 contaminated food while preventing excessive viral accumulation, flies from the different
74 persistently infected lines were transferred to new food every other day. Persistent viral
75 infections significantly reduce the survival of infected flies, as previously described
76 (Figure 1B; Nigg *et al.,* 2024). DAV infection has the most pronounced effects on survival,
77 followed by DCV, Bloomfield virus, and Nora virus (Mantel-Cox test infected vs uninfected
78 $P < 0.001$ for all the virus-infected populations). This is reflected by the time at which 50%
79 of the population has perished, the median survival (Figure 1B): 25 days post-eclosion
80 (dpe) for DAV, 28 dpe for DCV, 36 dpe for Bloomfield virus, and 52 dpe for Nora virus,
81 compared to 63 dpe for uninfected flies. This information enabled us to establish
82 different time points for further characterization of the infections: 1 dpe as an early time
83 point, 12 dpe as an intermediate time point just before the onset of virus-induced
84 mortality and the median survival as a late time point specific for each condition.
85 Additionally, we added an additional time point for DCV at 6 dpe, as mortality starts
86 earlier for this virus. In the present study, these time points served as the basis for
87 characterizing the impact of persistent viral infections on the physiology and behavior of
88 infected hosts (Figure 1A).

89 To characterize the dynamics of viral load within the infected populations, we
90 examined viral RNA levels in individual flies at the aforementioned early, intermediate,
91 and late stages of infection. Viral loads were quantified by RT-qPCR by measuring viral
92 RNA levels relative to the Drosophila housekeeping gene *Rp49*. Flies were classified as
93 infected if their Ct values for viral RNA were below 35 with melting temperature profiles
94 indicating the presence of a single amplicon. We observed distinct patterns of viral

accumulation for each virus (Figure 1C, upper panels). DAV exhibited a rapid increase in viral RNA levels early post-eclosion, with a median increasing by ~4 and ~5 log_{10} orders of magnitude at 12 and 25 dpe, respectively. In contrast, DCV displayed a relatively stable pattern in viral RNA levels over time, with no significant changes in viral loads. Interestingly, we noted that DCV-infected individuals stably clustered into two distinct groups, displaying viral RNA levels several orders of magnitude apart. Bloomfield virus RNA levels rose steadily over the lifetime of infected individuals, increasing by 1 and 2 log_{10} orders of magnitude at 12 and 36 dpe, respectively. In contrast, Nora virus RNA levels remained consistent at the earlier timepoint but rose significantly by ~3 log_{10} orders of magnitude by the final timepoint (GLM, letters over the conditions indicate grouping for multiple comparisons).

Our examination of viral RNA levels allowed us to estimate infection prevalence in the different populations over time (Figure 1C, lower panels). A viral infection is considered prevalent in a population if individuals continue to be infected over time, even as time progresses. DAV and Nora virus were consistently detected in 100% of individuals, except for a slight reduction in Nora virus prevalence at the later stage (~91% of individuals infected at 52 dpe). Bloomfield virus was highly prevalent in the population at all time points, although not all individuals were infected at any given time, and infection prevalence varied from ~91% to ~72%. DCV was detected in all individuals at 1 dpe, and its prevalence in the population progressively decreased over time, with only ~36% of the individuals infected at the latest time point.

119 **Persistent viral infections impact viable offspring production**

120 Persistent viral infections can reduce individual survival rates, which may consequently
121 affect the viability of the population over time. To understand the broader impact of these
122 infections, we investigated whether populations with a prevalent viral infection affect the
123 production of viable offspring, which we define as the number of progeny that
124 successfully emerge as adults. This metric is a crucial aspect of reproductive success
125 and population dynamics. Any impact on the production of viable offspring would
126 indicate that persistent infections influence additional critical biological traits related to
127 fitness beyond the previously observed reduction in survival.

128 To explore this, we selected 20 females and 20 males from each infected and
129 uninfected stock on the day of eclosion (0 dpe). Flies were allowed to mate for 24 hours,
130 after which the males were discarded. The females were then transferred into new vials
131 with food each day, and the viable offspring were counted as they emerged. The final
132 progeny number was counted and normalized based on the number of female flies laying
133 eggs in each vial.

134 Flies collected from DAV, DCV, Bloomfield virus, or Nora virus-infected populations
135 exhibited distinct patterns of offspring production compared to uninfected controls over
136 time (Figure 2A). Uninfected flies exhibited a peak in viable offspring production at 1 dpe
137 with 10.3 ± 2.02 (mean ± SD) adults emerging per female. This was followed by a gradual
138 decrease in offspring production until 6 dpe, after which the decline became more
139 pronounced, ultimately reaching zero by 16 dpe. Similarly, populations infected with DAV
140 and Bloomfield viruses also peaked in viable offspring production at 1 dpe, with averages
141 of 11.5 ± 2.07 and 11.6 ± 1.30, respectively. These infected populations also experienced
142 a sharp decline in offspring production after 6 dpe. However, the pattern of viable

143 offspring per female daily indicates that, at the early time points, DAV and Bloomfield
144 virus-infected populations produced more viable offspring per female than the
145 uninfected control population (GLMM, DAV P = 0.0223, Bloomfield P = 0.0309). In a
146 different way, the DCV-exposed flies displayed a unique pattern in viable offspring
147 production, surpassing the uninfected group only at later time points (GLMM, $P < 0.0001$).
148 In contrast, Nora virus-infected flies consistently produced fewer viable offspring
149 (GLMM, P = 0.0098), peaking at 4 dpe with an average of 5.28 ± 2.15 viable offspring
150 produced.

151 Studying both daily and cumulative offspring production offers a comprehensive
152 perspective on reproductive dynamics. Daily offspring production highlights short-term
153 effects and variability, while cumulative offspring production indicates overall
154 reproductive success throughout the female's lifespan.

155 When examining the cumulative offspring per female, we see the total offspring
156 production from infected and uninfected stocks over time. We found that DCV-infected
157 flies produced more viable offspring (91.5 ± 32.1) than the uninfected group (67.7 ± 11.6)
158 (Figure 2B, GLMM, P = 0.0044). We also noted that Nora virus-infected flies produced
159 significantly fewer offspring per female (41.5 ± 15.5, GLMM, P = 0.0335). Overall, the
160 results illustrate the diverse and virus-specific impacts of persistent viral infections on
161 fertility.

162

163 **Persistent viral infections alter locomotor function in a virus-dependent manner**

164 Locomotor function is a key indicator of an organism's overall health and physiological
165 status. In flies, locomotion reflects both muscular and neurological capacity, making it a
166 valuable marker for assessing the general impact of viral infections on host physiology.

167 We assessed locomotor function using the reverse geotaxis assay, which measures
168 the flies' upward climbing instinct over a specified period (Gargano *et al.,* 2005). The
169 assay was performed on 20 mated females from different uninfected and infected stocks
170 at 1, 6, 12, and 20 dpe. This final time point was chosen as a common late date for all fly
171 stocks, occurring prior to the day of median survival for all of the infected populations.
172 Flies were placed in an empty tube and collected at the bottom by gently tapping the
173 tubes. After waiting for 3 seconds, a picture was taken, and the position of each fly was
174 recorded manually. Our observations indicated that persistent viral infections had a
175 mixed effect on locomotor function over time (Figure 3). DCV- and Nora virus-infected
176 flies consistently showed impaired locomotion abilities compared to uninfected flies at
177 almost all the tested time points (Figure 3A). In contrast, DAV- and Bloomfield-infected
178 flies showed mixed locomotion patterns. DAV significantly reduced mobility at 1 day
179 post-exposure (dpe) but significantly increased it at 6 and 20 dpe (GLMM, $P < 0.0001$, $P <$
180 0.0001, and $P = 0.0108$, respectively). Bloomfield virus significantly reduced mobility at 1
181 dpe and increased it at 12 dpe (GLMM, $P < 0.0001$ at both time points). When examining
182 the fly distribution patterns along the tubes we obtained similar results, with a higher
183 proportion of DCV- and Nora virus-infected flies found in the bottom of the tube at almost
184 all time points (Figure 3B). DAV infection resulted in a higher proportion of flies climbing
185 to the top of the tube at 6 dpe, but a higher proportion of flies at the bottom at 12 dpe
186 (CLMM, $P = 0.0008$ and $P = 0.0013$). Bloomfield virus-infected flies were found more often
187 on the bottom of the tube at 1 and 20 dpe, while they climbed more to the top at 12 dpe
188 (CLMM, $P < 0.0001$, $P = 0.0028$, and $P = 0.0322$, respectively). Taken together, these
189 results indicate that persistent viral infections affect the climbing abilities of infected
190 flies, with a general trend of lower climbing height, particularly in flies harboring Nora

191 virus infections. These findings underscore the systemic impact of persistent viral
192 infections on host physiology and behavior.
193
194 **Harboring persistent viral infections changes fly bacteriome composition**
195 We next investigated whether persistent viral infections influence the fly bacteriome—
196 the bacteria associated with the host. All fly populations in this study shared the same
197 genetic background and were reared under identical conditions, except for the presence
198 of different persistent viral infections. This controlled setup allowed us to attribute any
199 observed differences in the associated bacteria to the presence of different viral
200 infections.
201 Flies were collected at 12 dpe, surface sterilized and their DNA was extracted.
202 Microbiota composition was assessed by amplification and sequencing of the V3-V4
203 region of the *16S* rRNA bacterial gene. Although the microbiota of our flies was generally
204 dominated by *Lactobacillus* species, we detected changes in the relative bacterial
205 composition of infected flies compared to the uninfected control population.
206 Specifically, DAV- and DCV-infected flies showed an increase in the abundance of
207 *Lactobacillus*, while Nora virus infection increased the relative abundance of
208 *Sphingomonas* and *Thepidiphilus* genera (Figure 4). We are currently conducting
209 additional replicates and including Bloomfield virus in our analysis to further elucidate
210 the bacteriome changes induced by persistent viral infections. These ongoing studies will
211 provide a more comprehensive understanding of how different viruses influence the gut
212 microbial community and the potential implications for host physiology and fitness.
213
214

215 **Host transcriptional response is virus specific**

216 We observed that persistent infections are associated with modulations of the life history
217 traits discussed above. To gain insight into the host response to persistent viral infections,
218 we studied the transcriptional response of flies at early, intermediate, and late stages of
219 infection. For each time point and condition, we prepared four pools consisting of RNA
220 extracted from three to five individuals. These pools were prepared using the same RNA
221 samples used for the RT-qPCR analysis shown in Figure 1C. Informed by the RT-qPCR
222 data, we excluded non-infected individuals and randomly selected RNA from infected
223 individuals to prepare RNA pools for sequencing.

224 Observing the general transcriptomic profile of each condition, we found that each
225 enteric virus elicited a distinct transcriptional response in the host. Nora virus infection
226 was characterized by the most unique transcriptional response at 1 dpe (Supplementary
227 Figure 1), with the differential regulation of several genes (Supplementary Figure 2, 3). On
228 the contrary, at the same early time point other viruses induced little changes in
229 transcriptional profiles of infected flies and samples clustered together with uninfected
230 flies (Supplementary Figures 1-3). At a more advanced time point (12 dpe) the
231 transcriptional profiles of DCV and Bloomfield virus-infected flies clustered together with
232 uninfected flies, while Nora virus and DAV-infected flies were characterized by unique
233 transcriptional responses (Supplementary Figure 1). At the days of median survival, all
234 viruses induced significant changes in transcriptional profiles (Supplementary Figure 1).
235 Among viral infections at the same time points, no specific differentially expressed gene
236 (DEG) could be identified as a common factor across all infections (Supplementary
237 Figure 4). Furthermore, during a persistent infection, we could not identify a consistent
238 set of host genes that respond to the infection over time, thereby illustrating its

239 differential impacts as the infections progress (Supplementary Figure 4). Even when
240 comparing the transcriptomic profiles at the days of median survival, no common
241 transcriptional profile was shared among all infections (Supplementary Figure 4). We
242 also observed an increase in the number of DEGs as infection progressed for the flies
243 persistently infected with DAV, DCV, and Bloomfield virus (Supplementary Figures 3-4).
244 Many of the top DEGs identified within the diverse transcriptomic profiles at 1 dpe and 12
245 dpe are uncharacterized genes (Supplementary Figure 3).

246 Focusing on the genes known to participate in antiviral immune responses
247 (Supplementary File 1), Nora virus elicited the highest levels of upregulation and
248 downregulation at 1 dpe (Figure 5A). At 12 dpe, among the top twenty differentially
249 expressed genes (DEGs), DAV had the most genes upregulated. We found that DAV
250 infection resulted in the upregulation of genes associated with immune defense and
251 stress response pathways, indicating a potent antiviral response (Figure 5A). Conversely,
252 specific immune genes that appear upregulated during DAV infection are downregulated
253 during Nora virus infection. This applies to *PGRP-SC2*, the *Peptidoglycan Recognition*
254 *Protein SC2* gene, a negative regulator of the IMD pathway, and *PGRP-SC1a*, involved in
255 the Toll pathway signaling, as well as to *PGRP-SA* and *GNBP-like3,* involved in the Toll
256 pathway. This suggests that, although the immune response to these viruses may involve
257 some shared genes, it is fundamentally different, if not opposing (Figure 5A). Compared
258 to the other viruses, persistent DCV infection triggered the differential expression of a
259 modest set of immune genes; notably, the initial downregulation of *PGRP-SC1a* at 1 dpe
260 and a modest upregulation of immune genes as the infection progressed. Bloomfield
261 virus-infected flies also displayed initial downregulation of *PGRP-SC1a* at 1 dpe, followed
262 by an upregulation of *pirk* (IMD pathway) and *PGRP-SA* (Toll) (Figure 5A).

263 Upon analyzing the transcriptomic profiles of genes described to influence
264 locomotion (Supplementary File 1), we found that these genes were mostly notably
265 differentially expressed in Nora virus-infected flies at 1 dpe. Notably, *Lsp2,* a gene
266 reported to be involved in motor neuron axon and synaptic target inhibition (Inaki *et al.,*
267 2007), was upregulated in Nora virus-infected samples (Figure 5B). As infection
268 progresses, we observed an increasing number of DEGs related to locomotion, with Nora
269 virus infection showing an opposite transcriptional profile compared to DAV infection
270 (Figure 5B). At 12 dpe, Nora virus infection significantly upregulated *CG3857*, *Ptth*, and
271 *Rh5*, genes described to play roles in gravitaxis regulation, negative phototaxis, and light
272 reception, respectively (Armstrong *et al.,* 2006; Yamanaka *et al.,* 2013; Sprecher and
273 Desplan, 2008). In the same samples, we also observed an upregulation of genes related
274 to neuronal function, such as *nompC* and *Pdf* (Figure 5B) (Renn *et al.,* 1999; Walker *et al.,*
275 2000). Furthermore, Nora virus infection induced the upregulation of *M6*, a gene involved
276 in several neurological processes, including positive phototaxis and the downregulation
277 of *fz*, related to neuronal function, and *Neto*, a gene reported to not only have
278 neuromuscular roles but also to modulate hatching behavior (Kim *et al.,* 2012).
279 Conversely, for the DAV-infected samples, we observed an upregulation of *Neto*, along
280 with other genes like *esg* (related to stem cell maintenance and nervous system
281 development ; Bahrampour *et al.,* 2017; Biteau *et al.,* 2008; Hartl *et al.,* 2011) and *Mlc2*
282 (involved in flight ; Miller *et al.,* 2011) (Figure 5B). For the DCV-, and Bloomfield virus-
283 infected samples, we detected modest differential expression of locomotion genes.
284 Taken together, these results indicate that the host response to persistent infection is
285 virus specific.
286

287 **Viral infection induced transcriptional changes even after viral clearance**

288 Persistent viral infections, even if prevalent in the population and persistent in most
289 individuals, may still be cleared over time by the host (Figure 1B; Mondote *et al.,* 2018;
290 Nigg *et al.,* 2022). To investigate the long-term effects of viral clearance on the host, we
291 analyzed the transcriptome of flies that cleared the DCV infection (Figure 6). In fact, in the
292 DCV-infected population all individuals tested at 1 dpe were infected (Figure 1C), but
293 more than half of the population had cleared the infection by 28 dpe (Figure 1C).
294 Therefore, we analyzed the transcriptional response of flies that had cleared DCV
295 infection by 28 dpe and found that it remained significantly altered compared to the
296 never-infected control population (Figure 6A). We further explored the differences in the
297 transcriptomic profiles of DCV-infected and DCV-cleared flies. These results indicate
298 that only a few genes are differentially expressed between the two sets of samples (Figure
299 6B). Most of these genes were mitochondrial transfer RNAs, or genes encoding for
300 mitochondrial proteins, such as a subunit of the mitochondrial ATPase (*mt:ATPase8*), a
301 protein belonging to the cytochrome c oxidase assembly (*l(3)neo43*), a protein involved
302 in mitochondrial fatty acid beta-oxidation (*Mcad*), a mitochondrial single stranded DNA-
303 binding protein (*mtSSB*), a protein part of respiratory chain complex (*ND-MWFE*), a carrier
304 protein of the inner mitochondrial membrane (*sea*). The transcriptomic profiles of the two
305 sample groups showed significant changes when compared to the never-infected control
306 population. Specifically, genes related to the immune response continued to be
307 upregulated (Figure 6D). These results suggest that the host transcriptome does not
308 completely revert to its pre-infection state even after viral clearance, indicating lingering
309 effects on host physiology and immune function.

310

311 **DISCUSSION**

312 Our study provides a comprehensive examination of the impacts of persistent viral
313 infection on key biological traits in *D. melanogaster*. By studying mono-infections with
314 four different enteric RNA viruses, we reveal a complex interplay between viruses and
315 their hosts that affects survival, reproductive output (fertility), microbiota composition,
316 locomotor abilities, and transcriptional profiles.

317 We observed a trade-off between survival and reproductive output. This trade-off
318 suggests a compensatory mechanism in which, when faced with specific stressors such
319 as viral infections, the host organism may prioritize reproduction over immunity to ensure
320 population survival (Pontzer and McGrosky, 2022; Pagán *et al.,* 2008). Indeed, for DCV,
321 DAV, and Bloomfield viruses, we noted reduced survival but increased offspring
322 production in infected flies, indicating a redirection of resources from surviving the
323 infection to reproduction. Conversely, for Nora virus infections, resources appear to be
324 redirected primarily toward surviving the infection, as flies infected by this virus exhibit
325 the smallest impact on survival but a significant reduction in offspring production. These
326 diverse interactions correspond with the unique host transcriptional changes induced by
327 each virus. Notably, Nora virus causes a more substantial disruption to the
328 transcriptome, suggesting a higher immune investment in combating the infection. The
329 differing impacts on offspring production observed across various viral infections are
330 consistent with previous findings (Wallace and Obbard, 2024).

331 The viruses studied in this work are enteric viruses, meaning that they are transmitted
332 via the fecal-oral route, infecting the organism through the gut. Our observations show
333 that persistent enteric infections significantly shape the bacterial community present
334 within the flies, which is presumed to be located mainly within the gut. This finding agrees

335 with research focused on acute infections, wherein alterations in microbiome
336 composition have been observed across diverse hosts. The microbiome can modulate
337 immune responses, nutrient absorption, and overall host physiology and thereby affect
338 the outcome of viral infections (González and Elena, 2021; Schissel *et al.,* 2021). Hence,
339 some of the effects observed could be partially explained by the microbiota changes
340 induced by the viral infections. However, it has been observed that for infections with DAV
341 (Nigg *et al.,* 2024) and Nora virus (Franchet *et al.,* 2025), the relative impact on fly survival
342 is largely independent of the microbiota.

343 Despite the enteric nature of these infections, our observations indicate that their
344 impacts extend beyond the gut, as seen in the locomotion results. The effects on
345 locomotion reflect changes in metabolic and/or neurological status (Grotewiel *et al.,*
346 2005) and may have profound implications for fly behavior and ecology. Impaired
347 locomotion can affect activities such as foraging, mate searching, and dispersal,
348 consequently influencing the fly's ability to colonize new locations and disseminate
349 associated microbes. This has important implications for disease vectoring and the
350 spread of pathogens. The systemic impact of enteric infections in flies has also been
351 observed for enteric bacteria (Deshpande *et al.,* 2022). One potential explanation for this
352 is the virus spreading from its primary location in the gut to other tissues. Such spreading
353 has been documented for DCV (Ferreira *et al.,* 2014), DAV (Nigg *et al.,* 2024), Nora virus
354 (Franchet *et al.,* 2025). Further studies are required to understand the extent and
355 mechanisms of this dissemination. Another potential explanation for the systemic
356 effects of enteric infections is the dissemination of immune signaling molecules.
357 Molecules released in response to localized gut infections can have far-reaching effects
358 on distant organs and tissues. For instance, studies have shown that gut-derived

359 inflammatory signals can influence brain function and behavior, a phenomenon known
360 as the gut-brain axis (Cryan and Dinan, 2012; Mayer, 2011). This interorgan
361 communication can modulate various physiological processes, including metabolism,
362 immunity, and even cognitive function. Therefore, the systemic impacts of enteric viruses
363 may be mediated not only by direct viral spread but also by the immune signaling
364 molecules that circulate throughout the host.

365 Finally, we would like to acknowledge some limitations of our work. First, while all
366 individuals are infected at the time of eclosion, not all flies remain infected throughout
367 their adult lifespan, despite the virus remaining prevalent in the population. For DAV, Nora
368 virus, and Bloomfield virus, prevalence remained high, with approximately 100%, 92%,
369 and 72% of individuals remaining infected, respectively. In contrast, most individuals in
370 the DCV-infected population cleared the virus by the time of median survival.
371 Nevertheless, we observed lasting changes to the host transcriptome in flies that cleared
372 DCV, suggesting that DCV infection may cause long-lasting or permanent alterations in
373 host physiology and immune function. This is reminiscent of the long-lasting effects of
374 acute infections (Choutka *et al.,* 2022). Another limitation is that our study focused on
375 females of a single genetic background. Both sex and genetic background are known to
376 influence the effects of viral infections in Drosophila (Vale and Jardine, 2015; Klutzier *et*
377 *al.,* 2023)

378 In conclusion, our study demonstrates that persistent viral infections significantly
379 impact key biological traits in *D. melanogaster*. This adds to the growing evidence that
380 persistent infections profoundly impact host fitness and physiology.

381

382 **MATERIAL AND METHODS**

383 **Fly stock**

384 For all experiments we used *Wolbachia*-free w^{1118} flies maintained on a standard
385 cornmeal diet (Bloomington). All experiments were done at 25°C under a 12:12 light:dark
386 cycle.

387

388 **Viral infections**

389 Persistently infected flies were established following the method described by Nigg and
390 colleagues in 2022 and are the same stocks used in the work of Nigg and colleagues
391 (2024). The stocks were maintained at 25°C under a 12:12 light:dark cycle.

392

393 **Survival analysis**

394 Survival analyses of the flies coming from persistently infected stocks were conducted
395 using 20 female flies/replicate sorted at 1 dpe. Male and female flies were collected on
396 the day of eclosion and left to mate for 24 hours. Subsequently, only female flies were
397 sorted in new tubes containing 20 females each. Each tube was considered a biological
398 replicate and a total of nine biological replicates (from three independent experiments)
399 were analyzed. Survival was monitored daily by counting the number of dead flies in each
400 vial and flies were transferred to new vials every two days. Fly survival was assessed from
401 the day of adult eclosion until death.

402

403 **Viral quantification**

404 Individual female flies were collected in 300 µl of TRIzol reagent (Invitrogen, 15596026).
405 The samples were homogenized using a pestle, and RNA was extracted following

406 manufacturer's instructions, supplemented with GlycoBlue (Invitrogen, AM9516) during
407 the precipitation process. RNA concentrations were measured using the Qubit RNA BR
408 Assay Kit (Invitrogen, Q10211). RT was performed using random primers and Maxima H
409 Minus Reverse Transcriptase (Thermo scientific, EP0751) following manufacturer's
410 instructions. The resulting cDNA was diluted 1:10 with MiliQ water. The qPCR was
411 performed using Luminaris Color HiGreen qPCR Master Mix (Thermo Scientific, K0374).
412 The reactions were done in triplicates of 10 µl each and using the corresponding set of
413 primers for each virus (Supplementary Table 1). The cycling conditions were as follows: 2
414 minutes at 50°C, 10 minutes at 95°C, followed by 40 cycles of 15 seconds at 95°C and 60
415 seconds at 60°C. A standard melt curve analysis was performed after the cycling
416 protocol. For the analysis of the results, the threshold for viral RNA detection was set to
417 35 Ct (i.e. if a sample had Ct higher than 35 it was considered non infected). The Ct values
418 of the virus for a sample were normalized against the Ct value of the housekeeping gene
419 *Rp49* for that sample (ΔCt). The $2^{-\Delta Ct}$ values were calculated per sample and their $\log_{10}$
420 plotted.
421

422 **Viable offspring production**

423 To assess viable offspring production, 20 female and 20 male flies from infected or
424 uninfected stocks were left to mate in clean fly vials for 24 hours after eclosion. After this
425 period, males were discarded, and the mated females were transferred to new tubes
426 every day until no more progeny was produced (17 days). All tubes were kept at 25 °C
427 under a 12:12 light:dark cycle, and the number of adult flies (i.e. the viable progeny) in
428 each tube was counted after 14 days. The number of offspring was normalized to the

429 number of adult females placed in each tube daily to account for those that did not
430 survive throughout the test duration.
431
432 **Climbing assays**
433 Climbing assays were performed following the method described by Barone and
434 Bohmann (2013). Briefly, a 9 cm empty tube was used, and 20 female flies were placed
435 inside. With the cotton cap on, tubes had a maximum climbable height of 7.2 cm. The
436 tubes were tapped three times over the span of three seconds, and the climbing height
437 was assessed by taking a picture 3 seconds after the last tap. Flies' height was assessed
438 manually on the pictures using a metric guide on the back of the tubes. For categorical
439 classification, flies were considered "Top" if they surpassed 6.2 cm, "Bottom" if they were
440 between 0.0-1.0 cm, and "Middle" if they were between 1.0 cm and 6.2 cm.
441
442 **Microbiota composition**
443 Female flies from uninfected or persistently infected stocks were collected at 12 dpe.
444 External microbes were removed by surface sterilization using subsequent washes in 10
445 % bleach for 5 min, 70 % ethanol for 5 min and three rinsing steps in sterile water. At least
446 20 flies per condition were collected in a single experiment. Flies were placed in a lysis
447 buffer (10 mM Tris-HCl (pH 8), 26 mM EDTA, 0.5% SDS, 5 mg/mL lysozyme) and
448 homogenized with sterile pestles. After incubating the lysates for 1 h at 37 °C, total DNA
449 was extracted using the DNeasy Blood & Tissue Kit (Qiagen) following the manufacturer's
450 instruction. The V3-V4 hypervariable region of the bacterial *16S* rRNA gene was amplified
451 using the primers 341F (5'-CCTACGGGNGGCWGCAG-3') and 805R (5'-
452 GACTACHVGGGTATCTAATCC-3'). Samples were amplified and sequenced at Microsynth

453 (Balgach, Switzerland) using Illumina MiSeq on paired-end mode. At least 104'000 reads
454 per sample were obtained. Analyses were performed using qiime 2 (version 2019.10).
455 After quality trimming, chimeras detection and for and rev read merging using dada2, at
456 least 75'000 reads per sample were obtained. Taxonomy was attributed to amplicon
457 sequence variants (ASVs) using the Silva classifier in qiime2. The resulting ASV table was
458 analyzed in R studio (version 4.2.1) using the phyloseq package (version 1.42.0).
459

460 **Transcriptome profiling by high-throughput sequencing**

461 For each condition, four samples were sequenced. Each sample was made by pooling
462 RNA from five individuals (3 ng of total RNA per individual), except for DCV at 28 dpe,
463 where the four pools were made from three individuals each. RNA-seq libraries were
464 prepared from 15 ng of pooled RNA using an NEBNext Ultra II RNA Library Prep Kit for
465 Illumina (New England Biolabs, E7770L) with NEBNext Multiplex Oligos for Illumina (Dual
466 Index Primers Set 1) (New England Biolabs, E7600S). All sequencing was performed on
467 an Illumina NextSeq 500 instrument using a NextSeq 500/550 High Output Kit v2.5 (75
468 cycles) (Illumina, 20024906). Raw sequencing reads were mapped to the *D.*
469 *melanogaster* genome release dmel-r6.56 with STAR version 2.7.11b (Dobin et al 2013).
470 Feature counting was performed with HTSeq version 0.11.2. (Putri et al. 2022), and
471 differential gene expression analysis was performed with DESeq2 in R Studio (version
472 2023.03.1). Log2 fold changes were transformed into Z-scores using the "ashr" package,
473 and only adjusted p-values were considered for analysis.
474
475
476

Statistical analysis

All statistical analyses were conducted using R version 3.6.1 within the Rstudio development environment version 2024.04.2+764. The level of significance was set at $P < 0.05$ and symbols indicate the significance of differences between conditions: *** $P < 0.001$; ** $P < 0.01$; * $0.01 < P < 0.05$.

To account for the block effect, we employed linear mixed-effects or general linear mixed-effects models. Generalized linear models (GLM) were fitted to the data using the g*lm f*unction from the “stats” package. Generalized linear mixed models (GLMM) were fitted to the data using the *lmer f*unction from the “lme4” package version 1.1-35.5 . Cumulative link mixed models (CLMM) using the *clmm* function from the “ordinal” package version 2023.12-4.1. Post hoc pairwise comparisons were performed using the *emmeans* function from the “emmeans” package version 1.10.5. Tukey’s or FDR correction were used to adjust for multiple comparisons. The letter-based grouping for pair-wise comparisons was created using the the *cld* function from the “multcomp” package version 1.4-26. The specific statistical methods applied to each figure are detailed in the legend of the corresponding figure.

493 **REFERENCES**

494 Armstrong JD, Texada MJ, Munjaal R, Baker DA, Beckingham KM. Gravitaxis in
495 *Drosophila melanogaster*: a forward genetic screen. Genes Brain Behav. 2006;5: 222–
496 239. doi:10.1111/j.1601-183X.2005.00154.x

497 Bahrampour S, Gunnar E, Jonsson C, Ekman H, Thor S. Neural Lineage Progression
498 Controlled by a Temporal Proliferation Program. Dev Cell. 2017;43: 332-348.e4.
499 doi:10.1016/j.devcel.2017.10.004

500 Barone MC, Bohmann D. Assessing Neurodegenerative Phenotypes in *Drosophila*
501 Dopaminergic Neurons by Climbing Assays and Whole Brain Immunostaining. JoVE.
502 2013; 50339. doi:10.3791/50339

503 Biteau B, Hochmuth CE, Jasper H. JNK Activity in Somatic Stem Cells Causes Loss of
504 Tissue Homeostasis in the Aging *Drosophila* Gut. Cell Stem Cell. 2008;3: 442–455.
505 doi:10.1016/j.stem.2008.07.024

506 Choutka J, Jansari V, Hornig M, Iwasaki A. Unexplained post-acute infection
507 syndromes. Nat Med. 2022;28: 911–923. doi:10.1038/s41591-022-01810-6

508 Crone EE. Is survivorship a better fitness surrogate than fecundity? Evolution. 2001;55:
509 2611–2614. doi:10.1111/j.0014-3820.2001.tb00773.x

510 Cryan JF, Dinan TG. Mind-altering microorganisms: the impact of the gut microbiota on
511 brain and behaviour. Nat Rev Neurosci. 2012;13: 701–712. doi:10.1038/nrn3346

512 Deshpande R, Lee B, Grewal SS. Enteric bacterial infection in *Drosophila* induces
513 whole-body alterations in metabolic gene expression independently of the immune

deficiency signaling pathway. Tennessen J, editor. G3. 2022;12: jkac163. doi:10.1093/g3journal/jkac163

Dobin A, Davis CA, Schlesinger F, Drenkow J, Zaleski C, Jha S, et al. STAR: ultrafast universal RNA-seq aligner. Bioinform. 2013;29: 15–21. doi:10.1093/bioinformatics/bts635

Ferreira ÁG, Naylor H, Esteves SS, Pais IS, Martins NE, Teixeira L. The Toll-Dorsal Pathway Is Required for Resistance to Viral Oral Infection in *Drosophila*. Schneider DS, editor. PLoS Pathog. 2014;10: e1004507. doi:10.1371/journal.ppat.1004507

Franchet A, Haller S, Yamba M, Barbier V, Thomaz-Vieira A, Leclerc V, et al. Nora virus proliferates in dividing intestinal stem cells and sensitizes flies to intestinal infection and oxidative stress. bioRxiv. 2025. doi:10.1101/2025.01.30.635658

Gargano J, Martin I, Bhandari P, Grotewiel M. Rapid iterative negative geotaxis (RING): a new method for assessing age-related locomotor decline in *Drosophila*. Exp Gerontol. 2005;40: 386–395. doi:10.1016/j.exger.2005.02.005

Goic B, Saleh M-C. Living with the enemy: viral persistent infections from a friendly viewpoint. Curr Opin Microbiol. 2012;15: 531–537. doi:10.1016/j.mib.2012.06.002

González R, Elena SF. The Interplay between the Host Microbiome and Pathogenic Viral Infections. mBio. 2021;12: e02496-21. doi:10.1128/mBio.02496-21

Gould AL, Zhang V, Lamberti L, Jones EW, Obadia B, Korasidis N, et al. Microbiome interactions shape host fitness. Proc Natl Acad Sci USA. 2018;115. doi:10.1073/pnas.1809349115

535 Grotewiel MS, Martin I, Bhandari P, Cook-Wiens E. Functional senescence in
536 *Drosophila melanogaster*. Ageing Res Rev. 2005;4: 372–397.
537 doi:10.1016/j.arr.2005.04.001

538 Hartl M, Loschek LF, Stephan D, Siju KP, Knappmeyer C, Kadow ICG. A New Prospero
539 and microRNA-279 Pathway Restricts CO2 Receptor Neuron Formation. J Neurosci.
540 2011;31: 15660–15673. doi:10.1523/JNEUROSCI.2592-11.2011

541 Ho T, Tzanetakis IE. Development of a virus detection and discovery pipeline using next
542 generation sequencing. Virology. 2014;471–473: 54–60. doi:10.1016/j.virol.2014.09.019

543 Inaki M, Yoshikawa S, Thomas JB, Aburatani H, Nose A. Wnt4 Is a Local Repulsive Cue
544 that Determines Synaptic Target Specificity. Curr Biol. 2007;17: 1574–1579.
545 doi:10.1016/j.cub.2007.08.013

546 Irschick DJ, Garland T. Integrating Function and Ecology in Studies of Adaptation:
547 Investigations of Locomotor Capacity as a Model System. Annu Rev Ecol Syst. 2001;32:
548 367–396. doi:10.1146/annurev.ecolsys.32.081501.114048

549 Jia Y, Jin S, Hu K, Geng L, Han C, Kang R, et al. Gut microbiome modulates *Drosophila*
550 aggression through octopamine signaling. Nat Commun. 2021;12: 2698.
551 doi:10.1038/s41467-021-23041-y

552 Kapun M, Barrón MG, Staubach F, Obbard DJ, Wiberg RAW, Vieira J, et al. Genomic
553 Analysis of European *Drosophila melanogaster* Populations Reveals Longitudinal
554 Structure, Continent-Wide Selection, and Previously Unknown DNA Viruses. Falush D,
555 editor. Mol Biol Evol. 2020;37: 2661–2678. doi:10.1093/molbev/msaa120

556 Kim Y-J, Bao H, Bonanno L, Zhang B, Serpe M. *Drosophila* Neto is essential for
557 clustering glutamate receptors at the neuromuscular junction. Genes Dev. 2012;26: 974–
558 987. doi:10.1101/gad.185165.111

559 Kutzer MAM, Gupta V, Neophytou K, Doublet V, Monteith KM, Vale PF. Intraspecific
560 genetic variation in host vigour, viral load and disease tolerance during Drosophila C virus
561 infection. Open Biol. 2023;13: 230025. doi:10.1098/rsob.230025

562 Mayer EA. Gut feelings: the emerging biology of gut–brain communication. Nat Rev
563 Neurosci. 2011;12: 453–466. doi:10.1038/nrn3071

564 Miller MS, Farman GP, Braddock JM, Soto-Adames FN, Irving TC, Vigoreaux JO, et al.
565 Regulatory Light Chain Phosphorylation and N-Terminal Extension Increase Cross-Bridge
566 Binding and Power Output in *Drosophila* at In Vivo Myofilament Lattice Spacing. Biophys
567 J. 2011;100: 1737–1746. doi:10.1016/j.bpj.2011.02.028

568 Mondotte JA, Gausson V, Frangeul L, Blanc H, Lambrechts L, Saleh M-C. Immune
569 priming and clearance of orally acquired RNA viruses in *Drosophila*. Nat Microbiol.
570 2018;3: 1394–1403. doi:10.1038/s41564-018-0265-9

571 Nigg JC, Castelló-Sanjuán M, Blanc H, Frangeul L, Mongelli V, Godron X, et al. Viral
572 infection disrupts intestinal homeostasis via Sting-dependent NF-κB signaling in
573 Drosophila. Curr Biol. 2024;34: 2785-2800.e7. doi:10.1016/j.cub.2024.05.009

574 Nigg JC, Mongelli V, Blanc H, Saleh M-C. Innovative Toolbox for the Quantification of
575 Drosophila C Virus, Drosophila A Virus, and Nora Virus. J Mol Biol. 2022;434: 167308.
576 doi:10.1016/j.jmb.2021.167308

Pontzer H, McGrosky A. Balancing growth, reproduction, maintenance, and activity in evolved energy economies. Curr Biol. 2022;32: R709–R719. doi:10.1016/j.cub.2022.05.018

Putri GH, Anders S, Pyl PT, Pimanda JE, Zanini F. Analysing high-throughput sequencing data in Python with HTSeq 2.0. Boeva V, editor. Bioinform. 2022;38: 2943–2945. doi:10.1093/bioinformatics/btac166

Renn SCP, Park JH, Rosbash M, Hall JC, Taghert PH. A pdf Neuropeptide Gene Mutation and Ablation of PDF Neurons Each Cause Severe Abnormalities of Behavioral Circadian Rhythms in *Drosophila*. Cell. 1999;99: 791–802. doi:10.1016/S0092-8674(00)81676-1

Schissel M, Best R, Liesemeyer S, Tan Y-D, Carlson DJ, Shaffer JJ, et al. Effect of Nora virus infection on native gut bacterial communities of *Drosophila melanogaster*. AIMS Microbiol. 2021;7: 216–237. doi:10.3934/microbiol.2021014

Shin SC, Kim S-H, You H, Kim B, Kim AC, Lee K-A, et al. *Drosophila* Microbiome Modulates Host Developmental and Metabolic Homeostasis via Insulin Signaling. Science. 2011;334: 670–674. doi:10.1126/science.1212782

Sprecher SG, Desplan C. Switch of rhodopsin expression in terminally differentiated *Drosophila* sensory neurons. Nature. 2008;454: 533–537. doi:10.1038/nature07062

Tafesh-Edwards G, Eleftherianos I. The role of *Drosophila* microbiota in gut homeostasis and immunity. Gut Microbes. 2023;15: 2208503. doi:10.1080/19490976.2023.2208503

Vale PF, Jardine MD. Sex-specific behavioural symptoms of viral gut infection and *Wolbachia* in *Drosophila melanogaster*. J Insect Physiol. 2015;82: 28–32. doi:10.1016/j.jinsphys.2015.08.005

Walker RG, Willingham AT, Zuker CS. A *Drosophila* Mechanosensory Transduction Channel. Science. 2000;287: 2229–2234. doi:10.1126/science.287.5461.2229

Wallace MA, Coffman KA, Gilbert C, Ravindran S, Albery GF, Abbott J, et al. The discovery, distribution, and diversity of DNA viruses associated with *Drosophila melanogaster* in Europe. Virus Evol. 2021;7: veab031. doi:10.1093/ve/veab031

Wallace MA, Obbard DJ. Naturally occurring viruses of *Drosophila* reduce offspring number and lifespan. Proc R Soc B. 2024;291: 20240518. doi:10.1098/rspb.2024.0518

Yamanaka N, Romero NM, Martin FA, Rewitz KF, Sun M, O'Connor MB, et al. Neuroendocrine Control of *Drosophila* Larval Light Preference. Science. 2013;341: 1113–1116. doi:10.1126/science.1241210

611 **FIGURES**

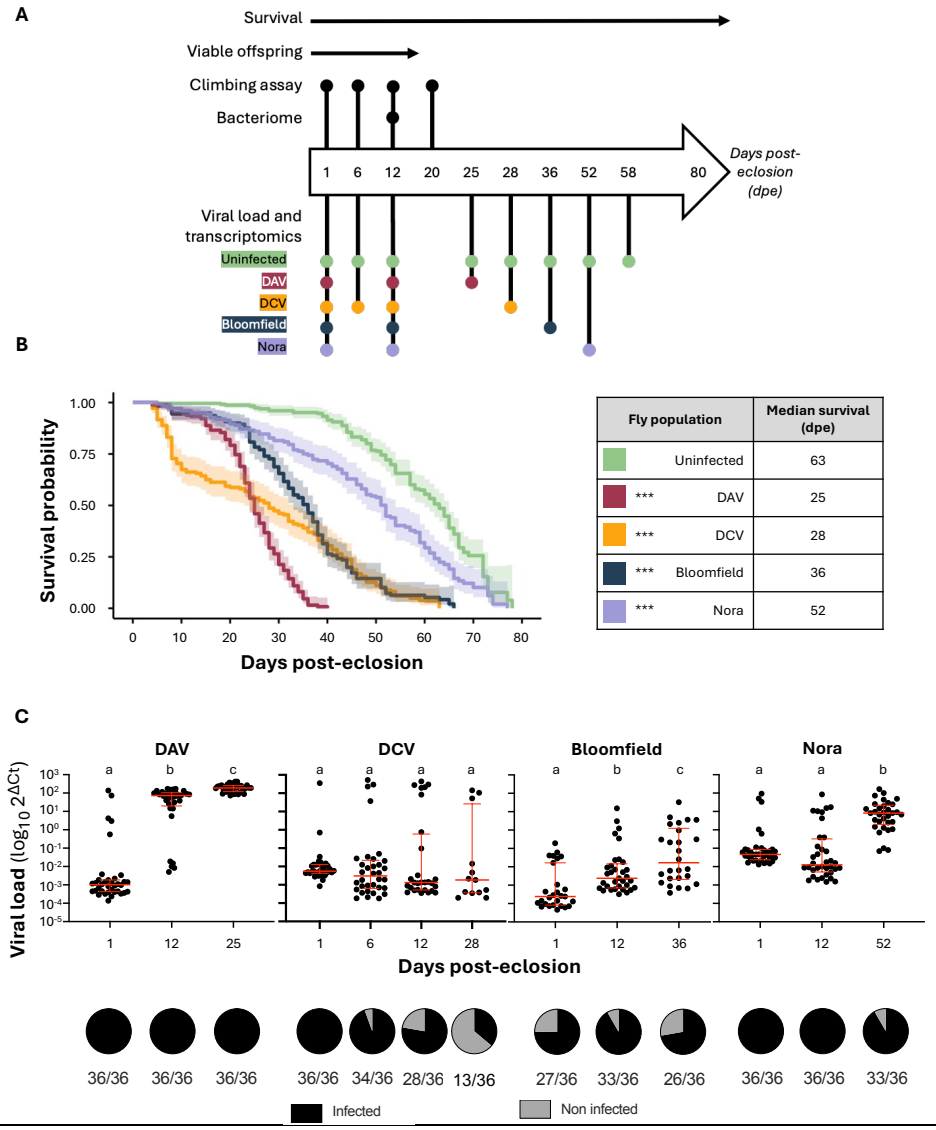

Figure 1. Experimental set-up, survival and viral dynamics of persistently infected fly population. ***A)*** *Experimental design. The large arrow indicates the days post-eclosion (dpe) during which specific experiments were conducted. The survival of persistently infected stocks has been monitored from eclosion until death across all stocks. The viability of offspring was assessed after a 24-hour mating period, until no more embryos were laid (17 dpe). Black dots indicate the specific days when the climbing assay and the sampling for the bacteriome studies were performed for all stocks. At the bottom of the graph, regarding the transcriptomics experiment, each colored dot signifies the date of sample collection for RNA sequencing corresponding to each different fly stock.* ***B)*** *Left panel shows the survival of w1118 flies uninfected (green) or persistently infected with DAV (red), DCV (yellow), Bloomfield virus (dark blue) or Nora virus (purple) Shaded regions indicate 95% confidence intervals. The data (n = 180 flies/condition in 3 independent experiments with 3 biological replcates/experiment) were obtained from Nigg et al. (2024). Statistical significance was assessed via the Mantel-Cox test. Right panel indicates the day post-eclosion at which 50% of the population is deceased.* ***C)*** *Viral infection dynamics. The upper panel shows viral RNA levels for DAV, DCV, Bloomfield virus, and Nora virus in infected populations. Viral RNA levels were measured in whole individuals at various times post-eclosion. Only data from infected individuals is presented. The Y-axis denotes the relative viral RNA level as* $\log_{10} 2^{\Delta Ct}$ *between the viral RNA and the housekeeping gene, Rp49. The red bars represent the median values along with the interquartile range*. For each virus, significance was calculated using a general linear model where the time point was the fixed factor; Tukey contrasts were used for post hoc analyses. Letters over the bars indicate letter-based grouping for multiple comparisons. Bottom panel: viral prevalence showing the proportion of flies resulting infected (black) or non-infected (grey) at the corresponding time-point. *Numbers below the pie chart represent the number of positives between the number of individuals sampled.*

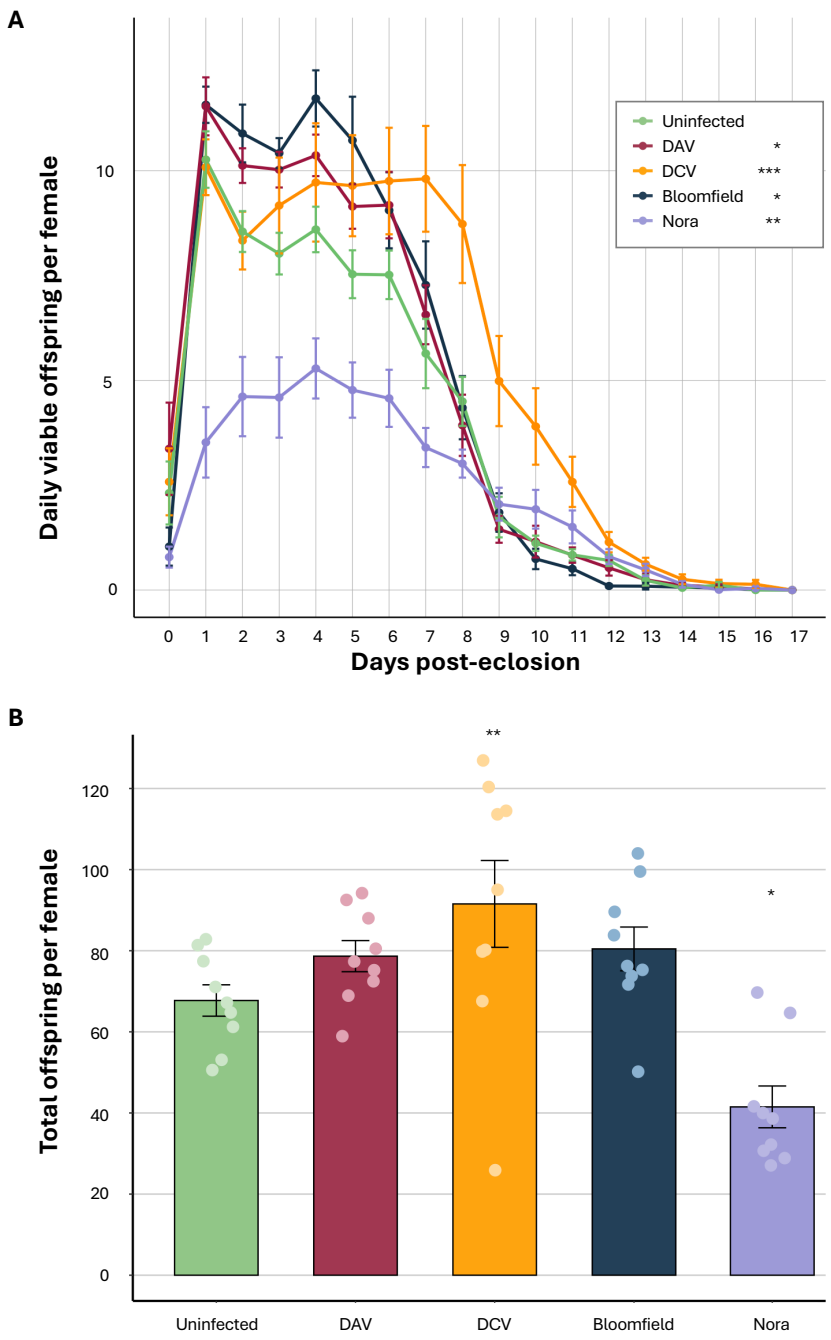

Figure 2. Impact of persistent viral infection on offspring production. ***A)*** *Daily viable offspring per female. Number of viable offspring produced by female flies uninfected (green) or persistently infected with DAV (red), DCV (yellow), Bloomfield virus (dark blue) or Nora virus (purple) after one day of mating (20 females paired with 20 males).* After one day, the males were discarded, and the females were transferred to new vials with food each day. Mated flies were kept for subsequent days, and the viable offspring were counted. *The number of viable offspring was normalized by the number of females laying eggs in each tube. Day 0 represents the day of eclosion and mating. Experiments were conducted on 20 females paired with 20 males in 9 replicates. Significance was calculated using a general linear-mixed model where the time point was the fixed factor and experiments a random effect; Tukey contrasts were used for post hoc analyses.* ***B)*** *Cumulative viable offspring shown in (**A**). Total viable offspring produced by each female was measured cumulatively across the different fly populations throughout the duration of the experiment. The Y-axis shows the total viable offspring per female and the X-axis the population studied. Significance was calculated using a general linear-mixed model where the virus status was the fixed factor and experiments a random effect; Tukey contrasts were used for post hoc analyses.*

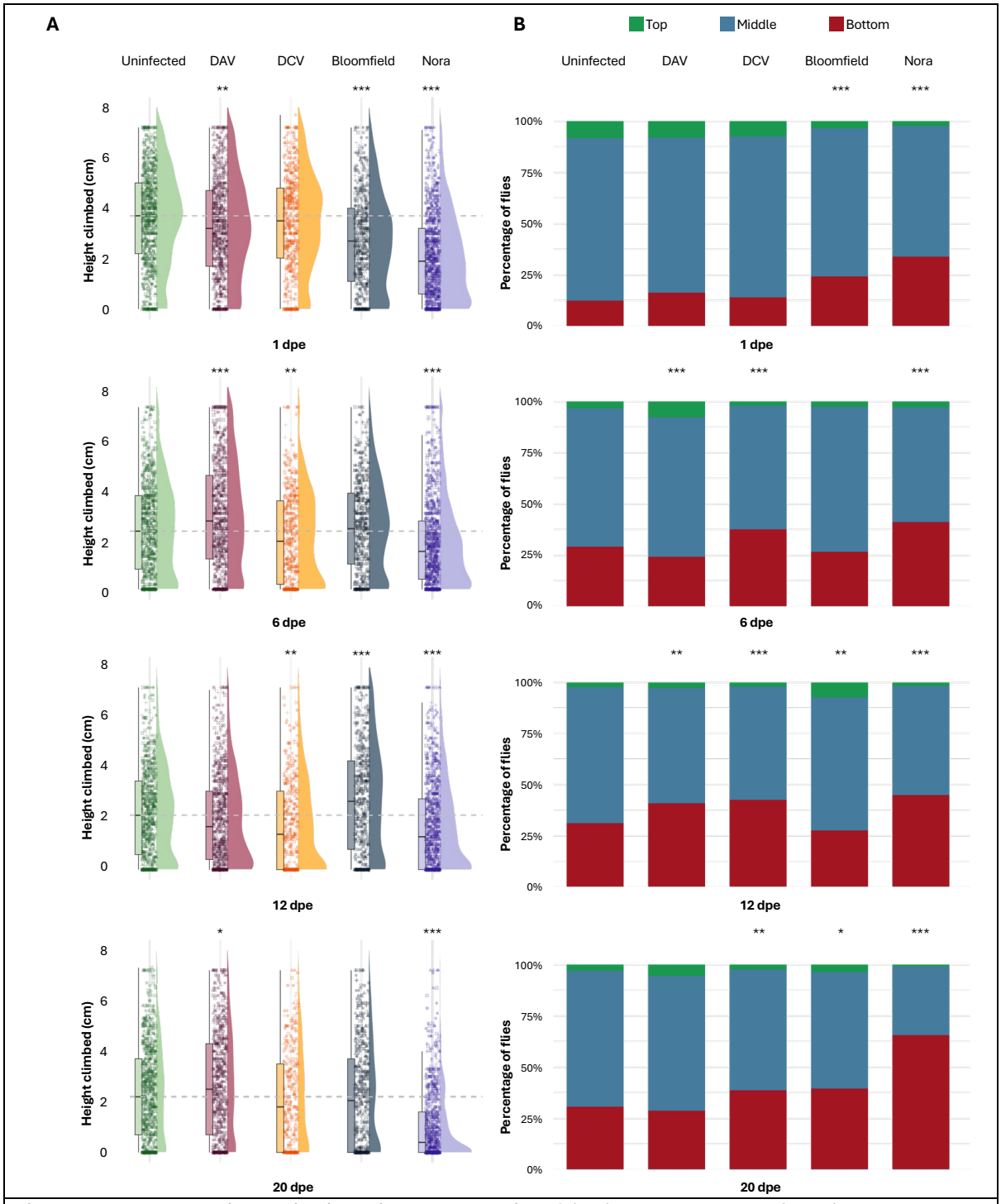

Figure 3. Impact of persistent viral infection on locomotion. *Climbing assay results of flies uninfected (green) or persistently infected with DAV (red), DCV (yellow), Bloomfield virus (dark blue) or Nora virus (purple).* ***A)*** *Quantitative height climbed by individual flies. Climbing assay results for days 1, 6, 12, and 20 post-eclosion. Results of 9 different biological replicates with 20 female flies. At each time point and replicate, six pictures were taken, and the height of each fly in the tube was recorded. Each symbol on the graph represents the recorded height of a fly for each picture. Boxplots are shown on the left side of each stock, indicating the median and interquartile range of the heights climbed by the flies. The dotted line represents the median height climbed by the uninfected population. The half-violin of each plot shows the density of the values. Significance was calculated using a general linear-mixed model where the virus status and the time point were the fixed factors and experiments a random effect; Tukey contrasts were used for post hoc analyses.* ***B)*** *Qualitative measurements of the climbing assay. Top (green) indicates the flies present in the top 1 cm of the climbing tubes (6.2-7.2 cm). Bottom (red) indicates the percentage of flies located in the bottom 1 cm of the tube (0-1 cm), and middle (blue) includes all flies that climbed between (1-6.2 cm). Significance was calculated using a cumulative link mixed model where the virus status and the time point were the fixed factors and experiments a random effect; false discovery rate contrasts were used for post hoc analyses.*

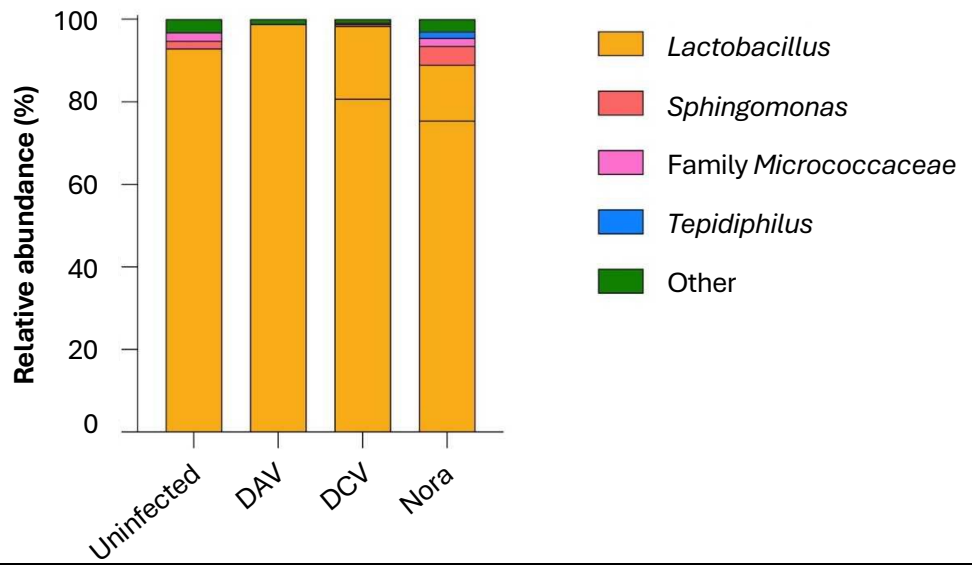

Figure 4. Bacteriome composition of the studied fly populations except for the one infected with Bloomfield virus. *Relative abundance in percentage of bacterial genera detected by sequencing of the V3-V4 region of the bacterial 16S rRNA gene. Each color corresponds to a specific bacterial genus sequenced in the microbiota. Bacteria belonging to different amplicon sequence variants (ASVs) but belonging to the same bacterial genus are displayed with the same color.*

612

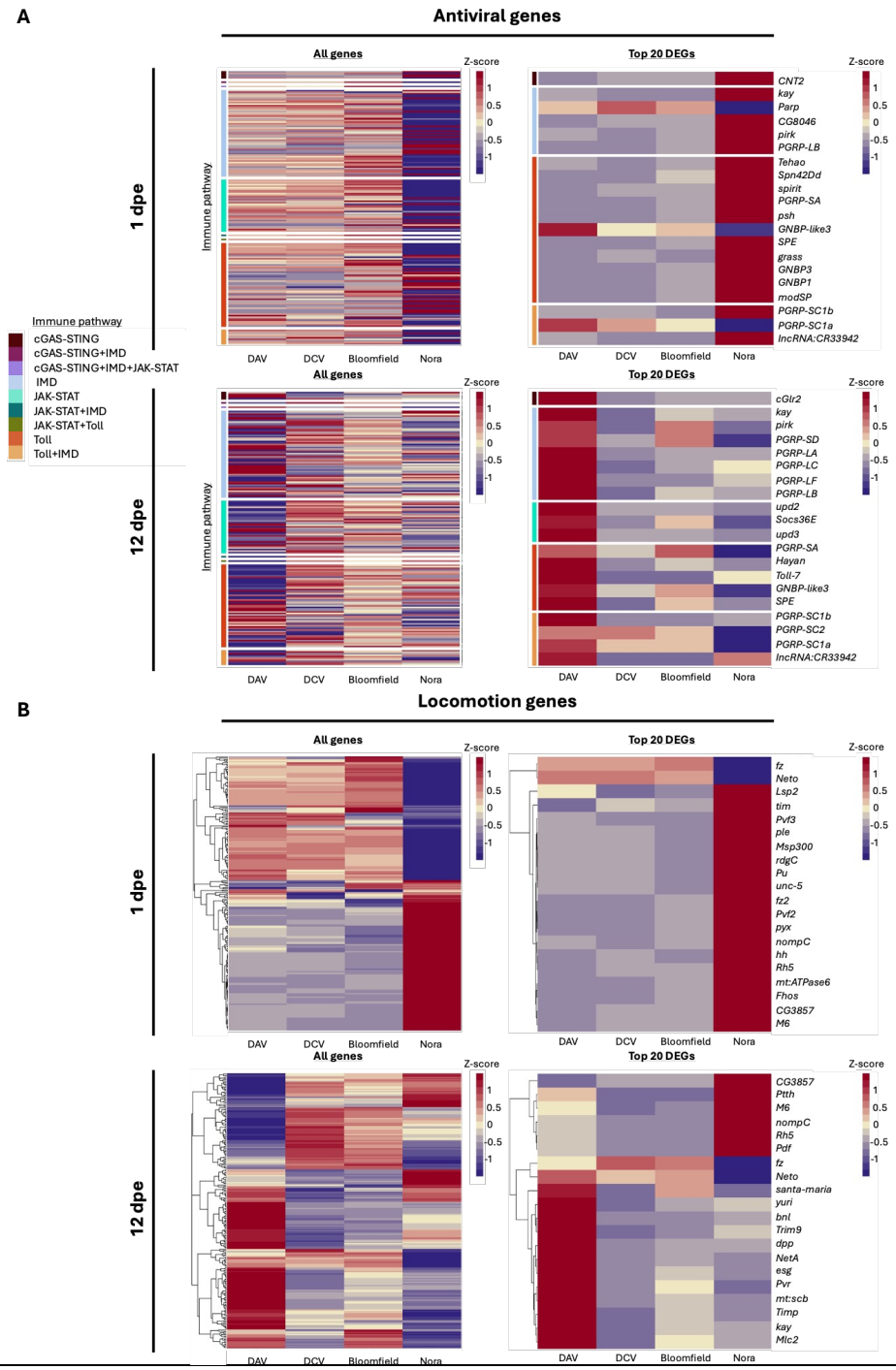

Figure 5. Transcriptomic profiles of uninfected or persistently infected flies. ***A)*** *Heatmaps expressing the Z-scores of gene expression fold change of infected populations in comparison with uninfected ones. Genes are represented in the Y-axis and the infecting virus on the X-axis. For each virus, the results are calculated on the average of 4 samples. Top left: heatmap showing all the genes reported to be involved in antiviral immunity (subset of 191 immune antiviral genes, Supplementary File 1) and their differential expression in our samples at dpe1. Top right: heatmap showing the top 20 differentially expressed immune genes at dpe1. Bottom left: heatmap showing all the genes reported to be involved in the insect's immune response and their differential expression in our samples at dpe12. Bottom right: heatmap showing the top 20 differentially expressed immune genes at dpe12. On the right side of each heatmap, a colored bar indicates the pathway in which the gene is reported to participate.* ***B)*** *Heatmaps showing all the genes reported to be involved in the insect's locomotion (a subset of 264 locomotion genes, Supplementary File 1) and their differential expression in our samples at dpe1. Top left: heatmap showing the top 20 differentially expressed locomotion genes at dpe1. Top right: heatmap showing all the genes reported to be involved in the insect's locomotion and their differential expression in our samples at dpe12. Bottom left: heatmap showing the top 20 differentially expressed immune genes at dpe12. Bottom right: heatmap showing the top 20 DEGs at dpe12.*

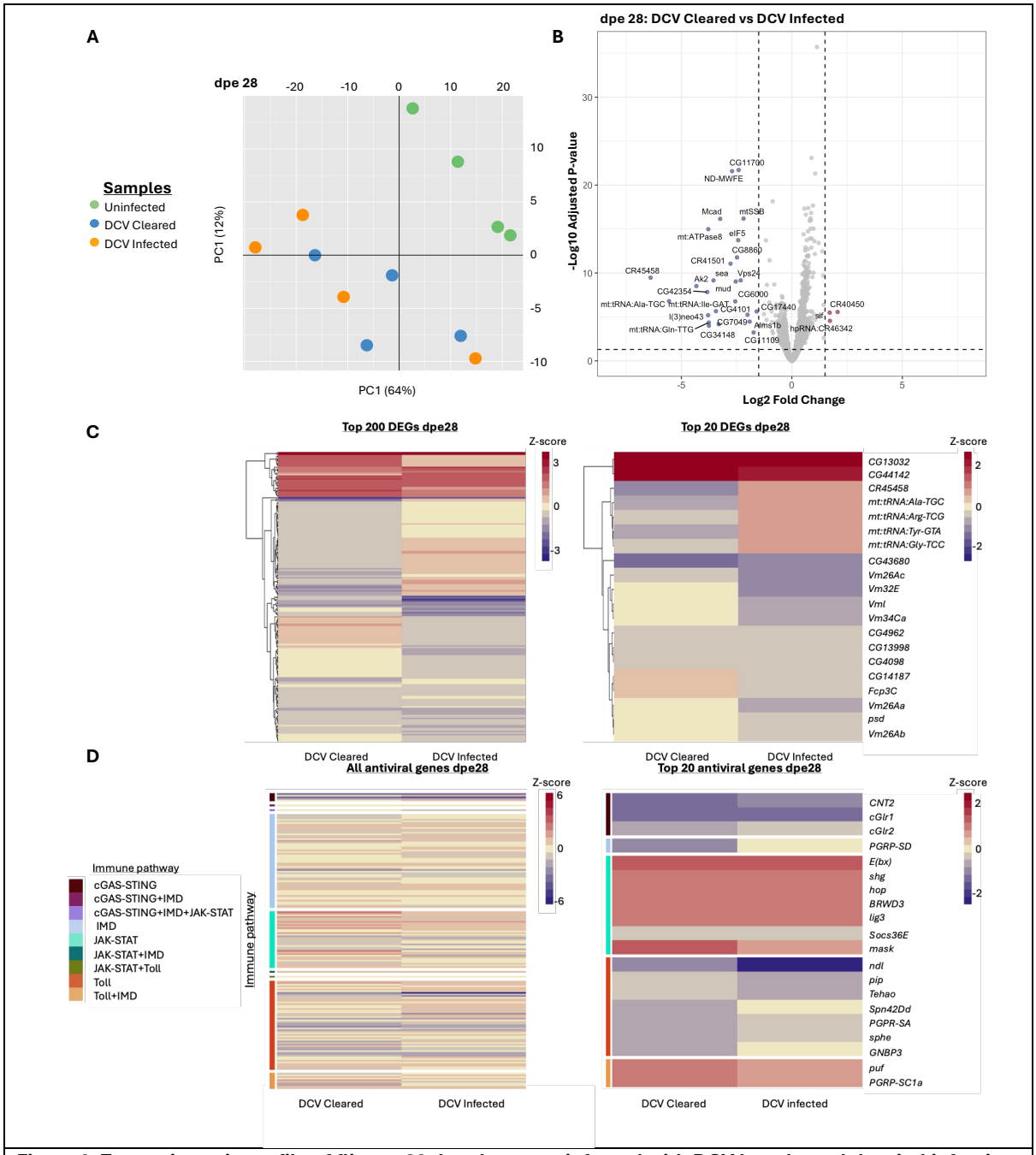

Figure 6. Transcriptomic profile of flies at 28 dpe that were infected with DCV but cleared the viral infection. ***A)*** *Principal component analysis of uninfected samples, DCV Infected, and DCV Cleared. On the X-axis, we indicate the first principal component (PC1) and the percentage of variance explained by this component in brackets.* ***On*** *the Y-axis, we indicate the second principal component (PC2) and the percentage of variance explained by this component in brackets.* ***B)*** *Volcano plot indicating the differentially expressed genes between DCV Cleared samples and DCV Infected ones. Genes significantly up- (in red) or down- (in blue) regulated. In grey, we represent those genes with differential expression values lower than 1.5 log2 fold change and p-adjusted values lower than 0.05. These thresholds are indicated by dotted lines in the graphs. The names of the DEGs are shown.* ***C)*** *Heatmaps representing the differential expression patterns between DCV Infected and DCV Cleared samples when compared to the Uninfected of the same age. Heatmap on the right shows the top 200 differentially expressed genes in our samples in terms of absolute log2 fold change value at dpe 28. Heatmap on the left shows the top 20 DEGs at dpe 28; gene names are indicated on the left.* ***D)*** *Heatmaps representing the differential expression patterns for reported immune genes between DCV Infected and DCV Cleared samples when compared to the Uninfected of the same age. Heatmap on the left shows all the genes reported to be involved in the insect's immune response and their differential expression in our samples at dpe 28. Heatmap on the right shows the top 20 differentially expressed immune genes at dpe 28; gene names are indicated on the left. On the right side of each heatmap, a colored bar indicates the pathway in which the gene is reported to involved.*

613 **SUPPLEMENTARY FIGURES**

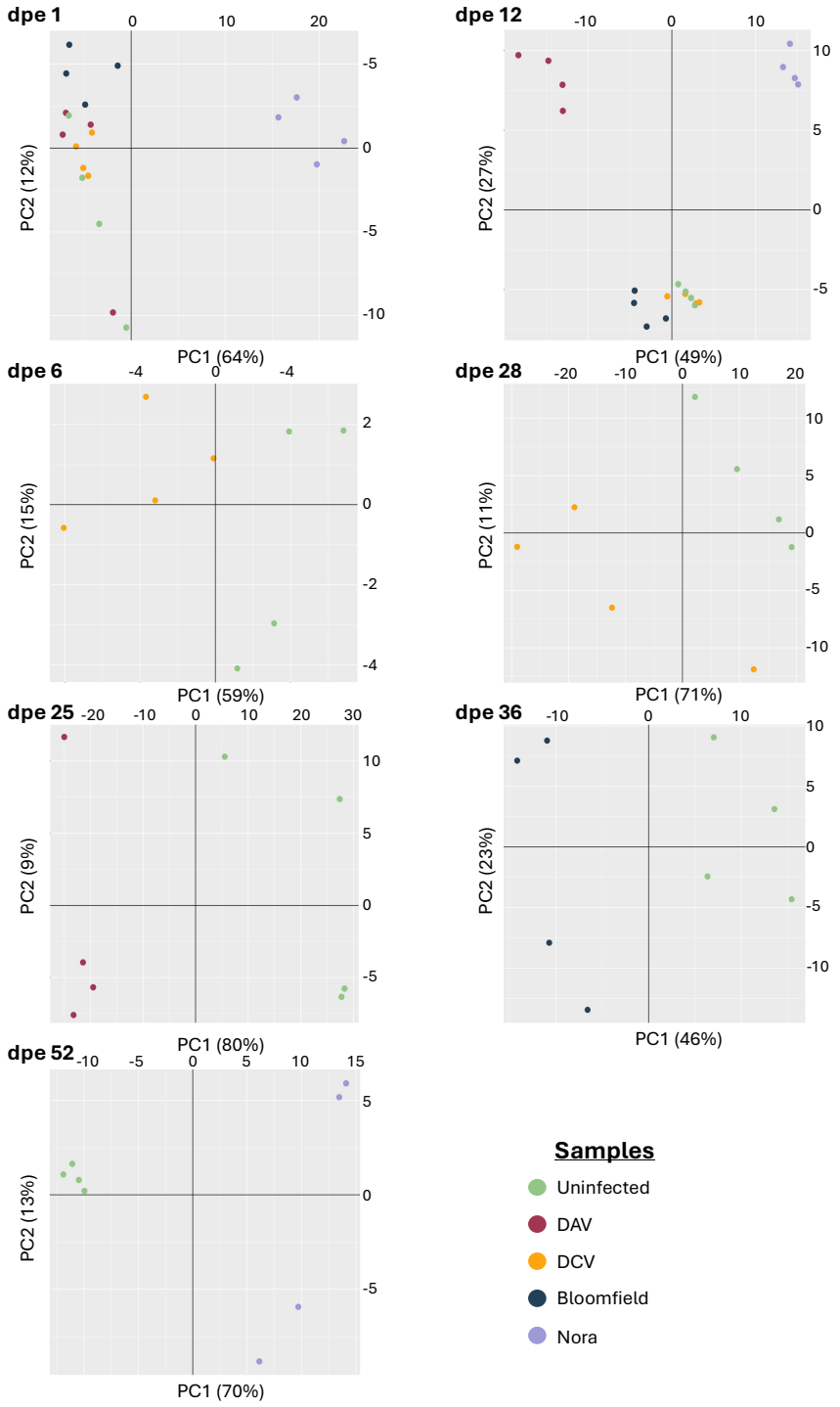

Supplementary Figure 1. *Principal Component Analysis of the different samples sequenced. On the Y axis of every graph, we indicate the second principal component (PC2) and the percentage of variance explained by this component between brackets. On the X axis, we indicate the first principal component (PC1) and the percentage of variance explained by this component between brackets. Black lines indicate the origin of each axis. The do represent our fly stocks throughout the different days post-eclosion, in green, we have the Uninfected stock, in burgundy, the Drosophila A virus persistent flies, in yellow, the Drosophila C virus persistently infected flies, in dark blue, we have the Bloomfield virus persistently infected stock, and in lavender the Nora virus persistently infected flies.*

614

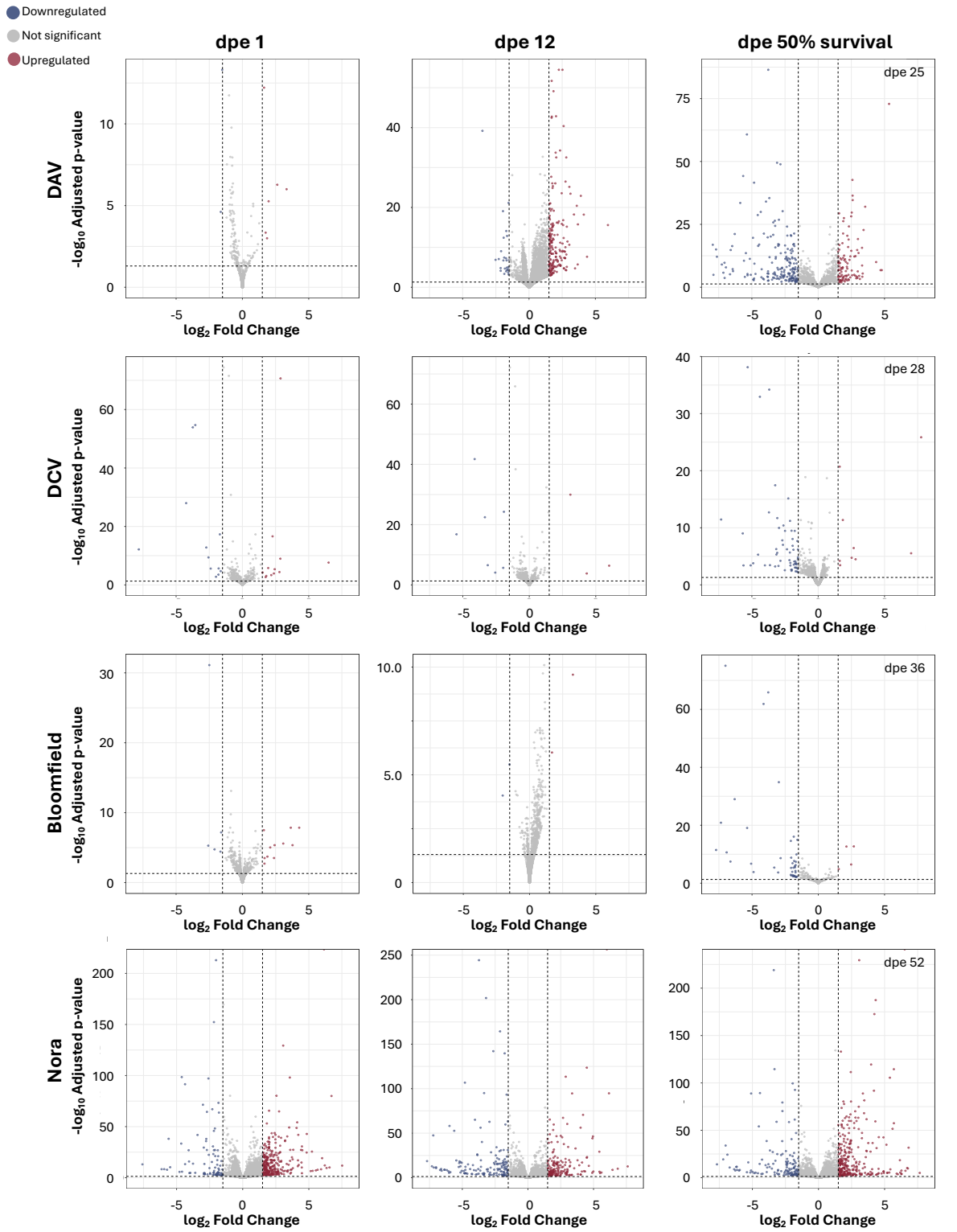

Supplementary Figure 2. *Transcriptomic results indicate differentially expressed genes in our infected samples. Volcano plots showing the number of genes significantly up- (in red) or down- (in blue) regulated. In grey, we represent those genes displaying differential expression values lower than 1.5 log2 fold change and/or with p-adjusted values lower than 0.05. These thresholds are indicated by dotted lines in the graphs. Each row presents the volcano plots of a specific fly stock over time (dpe), in the following order: DAV, DCV, Bloomfield, and Nora. Each infected sample is analysed in comparison to an uninfected control of the same age.*

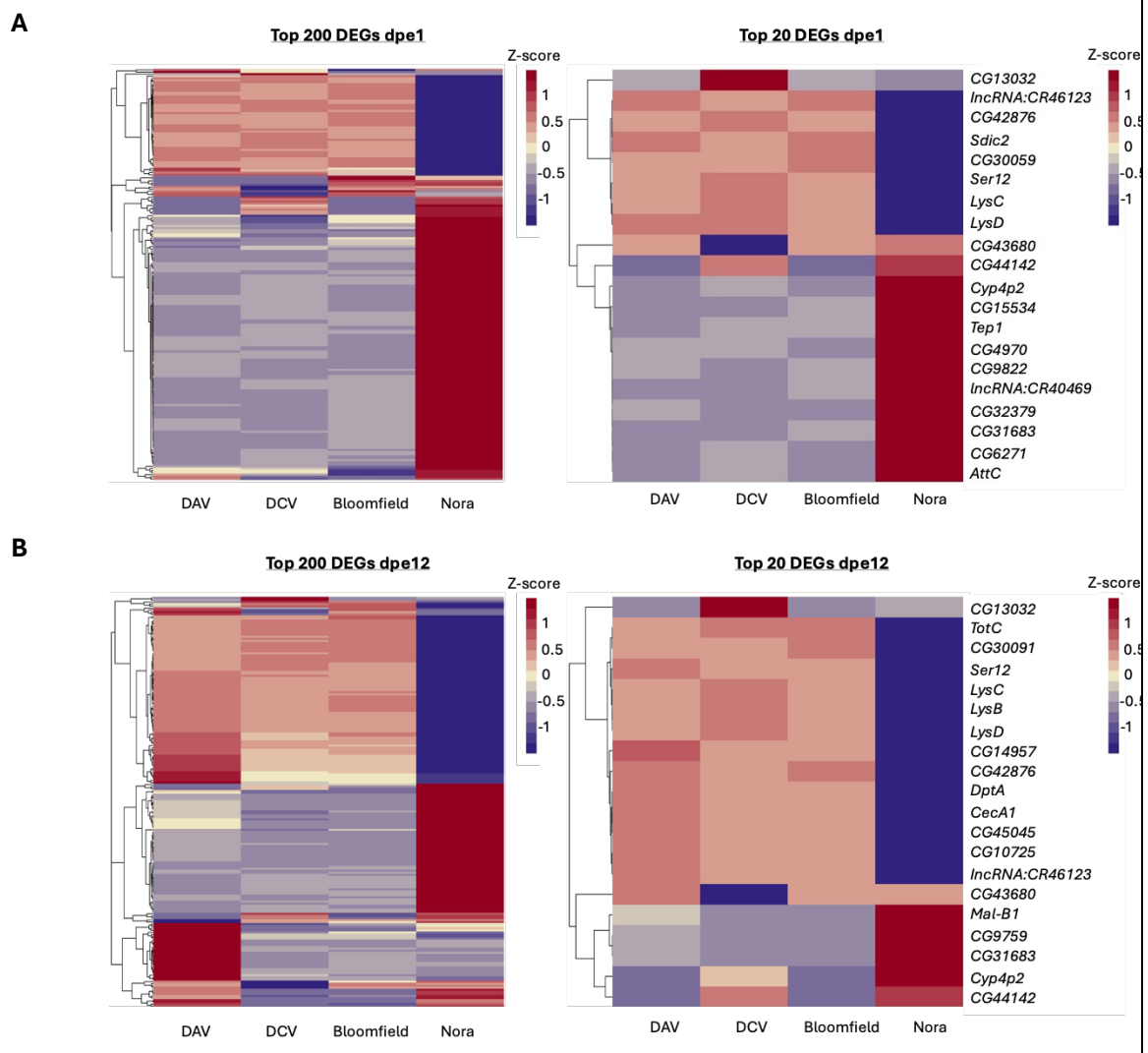

Supplementary Figure 3. *Persistent viral infection alters your transcriptomic profile in a virus-independent manner. For all heatmaps, on the X-axis, we indicate the infected stock analysed.* ***A)*** *From left to right: heatmap showing the top 200 differentially expressed genes in our samples in terms of absolute* log_2 *fold change value at dpe1. Heatmap showing the top 20 DEGs at dpe1.* ***B)*** *From left to right: heatmap showing the top 200 differentially expressed genes in our samples in terms of absolute* log_2 *fold change value at dpe12. Heatmap showing the top 20 DEGs at dpe12. For the heatmaps on the right, the top 20 gene names are indicated on the left of the graph.*

617

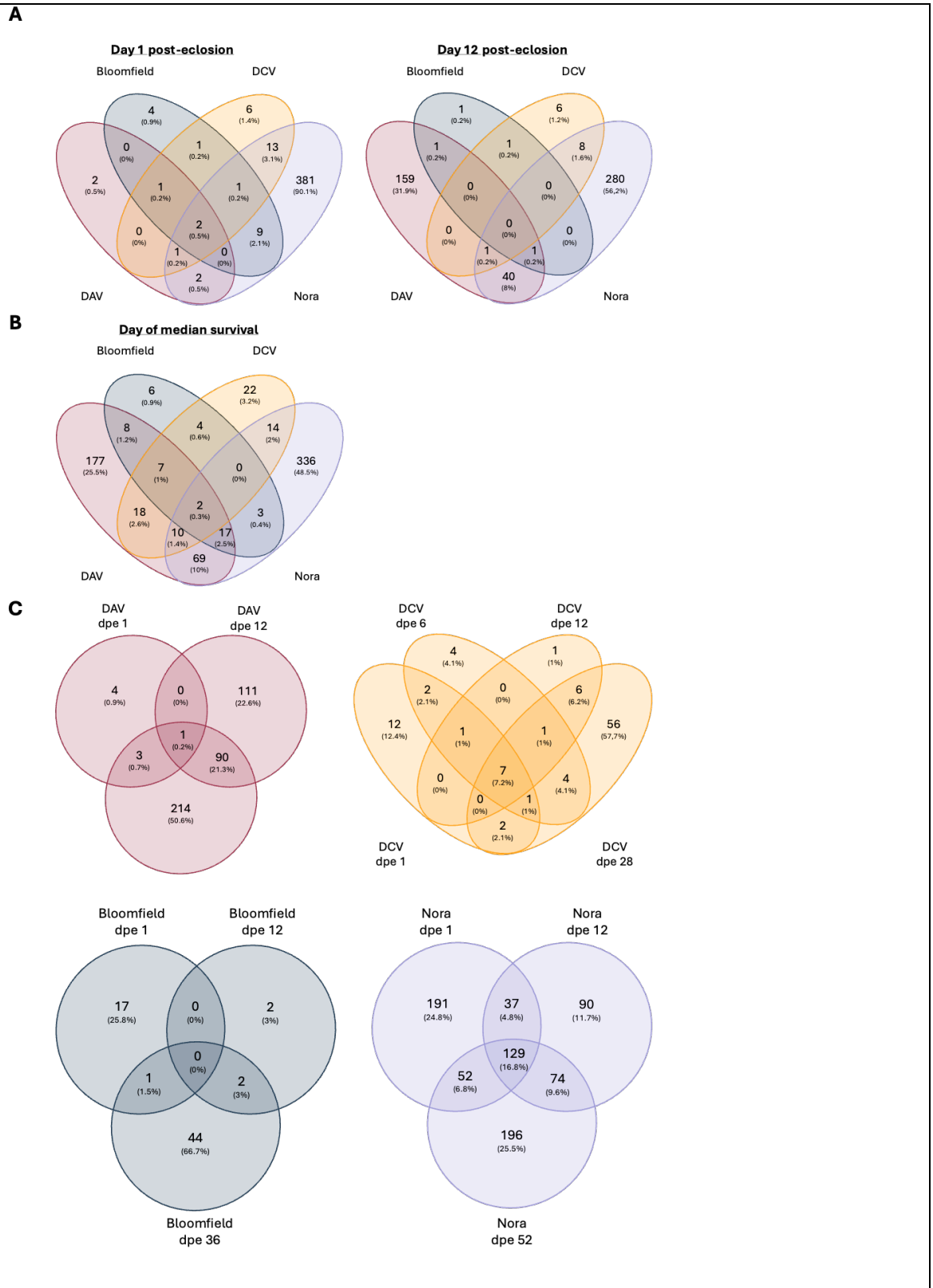

Supplementary Figure 4. *Common DEGs across infections and time. Venn diagrams of differentially expressed genes with differential expression values lower than 1.5 log2 fold change and/or with p-adjusted values lower than 0.05.* ***A)*** *DEGs for days 1, 12, and the day of median survival for each infected individual stock.* ***B)*** *DEGs on the day of median survival of all persistently infected stocks.* ***C)*** *DEGs for each persistently infected stock over time.*

618

619

620 **SUPPLEMENTARY TABLES**

621 **Supplementary Table 1.** Primers used in qPCR step of RT-qPCR for viral load

622 quantification.

Primer name	**Sequence**
Rp49_Forward	CGGATCGATATGCTAAGCTGT
Rp49_Reverse	GCGCTTGTTCGATCCGTA
DAV_Forward	GTTGGATCAGGCTAGTGTAGG
DAV_Reverse	TGCAACCGGACTCCAAGTTC
DCV_Forward	AGGCTGTGTTTGCGCGAAG
DCV_Reverse	AATGGCAAGCGCACACAATTA
Bloomfield_Forward	CCGCCGGCTACCTACTTTAG
Bloomfield_Reverse	ACCAGCAAGCGTCCGAAATA
Nora_Forward	GGTTTGCAGTTGATCGCAG
Nora_Reverse	TCAGCTCATCGTTCACGAA

623

624 **SUPPLEMENTARY FILES**

625 **Supplementary File 1.** Genes classified with antiviral immune or locomotion function.

626